Electronic Supplementary Material (ESI) for Environmental Science: Nano.

Electronic Supplementary Information

A Z-scheme $NiCo_2O_4$/S co-doped 1D g-C_3N_4 heterojunction for solar-light sensitive photocatalytic degradation of antibiotics in aqueous solutions exemplified by tetracycline

Thanh Binh Nguyen[a], Phung-Ngoc-Thao Ho[a], Chiu-Wen Chen[b], C.P. Huang[c], Ruey-an Doong[d], Cheng-Di Dong*[b]

[a] Institute of Aquatic Science and Technology, National Kaohsiung University of Science and Technology, Kaohsiung, 81157, Taiwan.

[b] Department of Marine Environmental Engineering, National Kaohsiung University of Science and Technology, Kaohsiung City, Taiwan.

[3] Department of Civil and Environmental Engineering, University of Delaware, Newark, 19716, DE, USA.

[d] Institute of Analytical and Environmental Sciences, National Tsing Hua University, Hsinchu, 30013, Taiwan.

---

* Corresponding author.

E-mail: cddong@nkust.edu.tw (Cheng-Di Dong)

S1. Characterization of catalysts

The crystalline phase of catalysts was identified by a powder X-ray diffractometer (D8 Advance, Bruker, Germany) with Ceramic XRD tube type KFL Cu Kα ($\lambda = 0.154$ nm) radiation over wide angle scanning range of 5-85^{o}. The morphology of the catalysts was imaged using a field emission scanning electron microscope (JSM-7800 Schottky FESEM, JEOL, USA) operated at an accelerating voltage of 10 kV for electron beam. Materials were sputter-coated with Pt by low vacuum Sputter Coater (MC1000 Hitachi, Tokyo) to reduce sample charging during FESEM measurement. Morphology and crystal structure was further obtained on F20 G2 MAT S-TWIN field emission gun transmission electron microscope (TEM, Tecnai, FEI Co).

The pore size distribution and Brunauer-Emmett-Teller (BET) surface area of catalysts were obtained from N_2 adsorption-desorption isotherm measured on a Micromeritics ASAP 2020 Physisorption (Norcross, GA, USA). Raman spectra were obtained using a confocal Raman microscope Senterra II (Bruker, Billerica, MA, USA) excited by a laser source of 10 W at a specific λ of 532 nm. The Fourier transform infrared (FTIR) spectra were collected on a Thermo Nicolet^{TM} iS10^{TM} -FTIR spectrometer (USA) in wavenumber range of 400−4000 cm^{-1} resolution through KBr pellet method. Thermal analysis was studied by a Mettler-Toledo TGA/DSC 3+ STAR (Schwerzenbach, Switzerland) at a heating temperature ramping rate of 10°C min^{-1} in the temperature range of 30−1000 °C under air atmosphere. Electron paramagnetic resonance (EPR) measurement was conducted on a Bruker EMXplust-10/12/P/L spectrometer (Bruker, Bremen, Germany) with microwave band frequency of 9.85 GHz and microwave power of 22.8 mW. The elemental composition of the catalysts was determined using Thermo ESCALAB 250Xi spectrometer (Waltham, MA, USA) controlled with an Al Kα monochromatized source at 15 kV and 15 mA. The pH of point zero charge (pH_{pzc}) of materials was determined by using Zetasizer Nano analyzer (Malvern Instrument, Worcestershire, UK).

S2 A*nalytical methods*

The residual TC concentration was analyzed using Hitachi HPLC Chromaster 5110 (Tokyo, Japan) equipped with a high-sensitivity UV-vis detector 5420 at the maximum absorption wavelength of 357 nm. TC in the solution was separated by using a reversed phase C18 column (Inertsil ODS-2, Si-$C_{18}H_{37}$, average diameter = 5 μm) and eluted with a binary mixture of 72% of oxalic acid 0.01 M, 20% acetonitrile and 8% of methanol at an isocratic flow rate of 1 $mL \cdot min^{-1}$. The samples (an accurate volume of 20 μL) were injected by Hitachi 5260 Autosampler. Total organic carbon (TOC) was determined with a TOC analyzer (O.I. Corporation, Aurora 1030W, Texas, USA). Chemical oxygen demand (COD) was analyzed according to Standard Methods (APHA, 1998). Inductively couple plasma mass spectrometry (ICP-MS) (Agilent 7500a, Santa Clara, CA USA) was used to determine the amount of cobalt in the solution. An ultra-high pressure liquid chromatography coupled with a mass spectrometer (UPLC® I-class IVD/Xevo® TQ-S micro IVD, Water Corporation, MA, USA) with a extend C_{18} column (2.1 x 50 mm 1.7 μm) was used to detect the byproducts of TC photodegradation. The mobile phase A was acetonitrile, and the mobile phase B was 0.1% formic acid in H_2O. The gradient elution procedure was $0 \rightarrow 1 \rightarrow 2 \rightarrow 3 \rightarrow 6 \rightarrow 7 \rightarrow 11 \rightarrow 12 \rightarrow 18$ min, the mobile phase A of acentontrile was $95\% \rightarrow 85\% \rightarrow 80\% \rightarrow 70\% \rightarrow 10\% \rightarrow 2\% \rightarrow 2\% \rightarrow 95\%$. The identification of the intermediates was carried out using the ESI positive ion mode. Source temperature was 150 ^{o}C. Desolvation temperature was 450 oC and the sheath gas flow rate was 650 L h^{-1}. The source voltage was set at 3500 V.

S2. Adsorption isotherm

The Langmuir model can be described as:

$$q_e = q_m \frac{K_L C_e}{1 + K_L C_e}$$

where: q_e is the equilibrium adsorption capacity of TC (mmol g^{-1}), q_m is the maximum monolayer adsorption capacity (mmol g^{-1}), K_L is the Langmuir constant (L $mmol^{-1}$), and C_e is the equilibrium TC concentration (mmol L^{-1}).

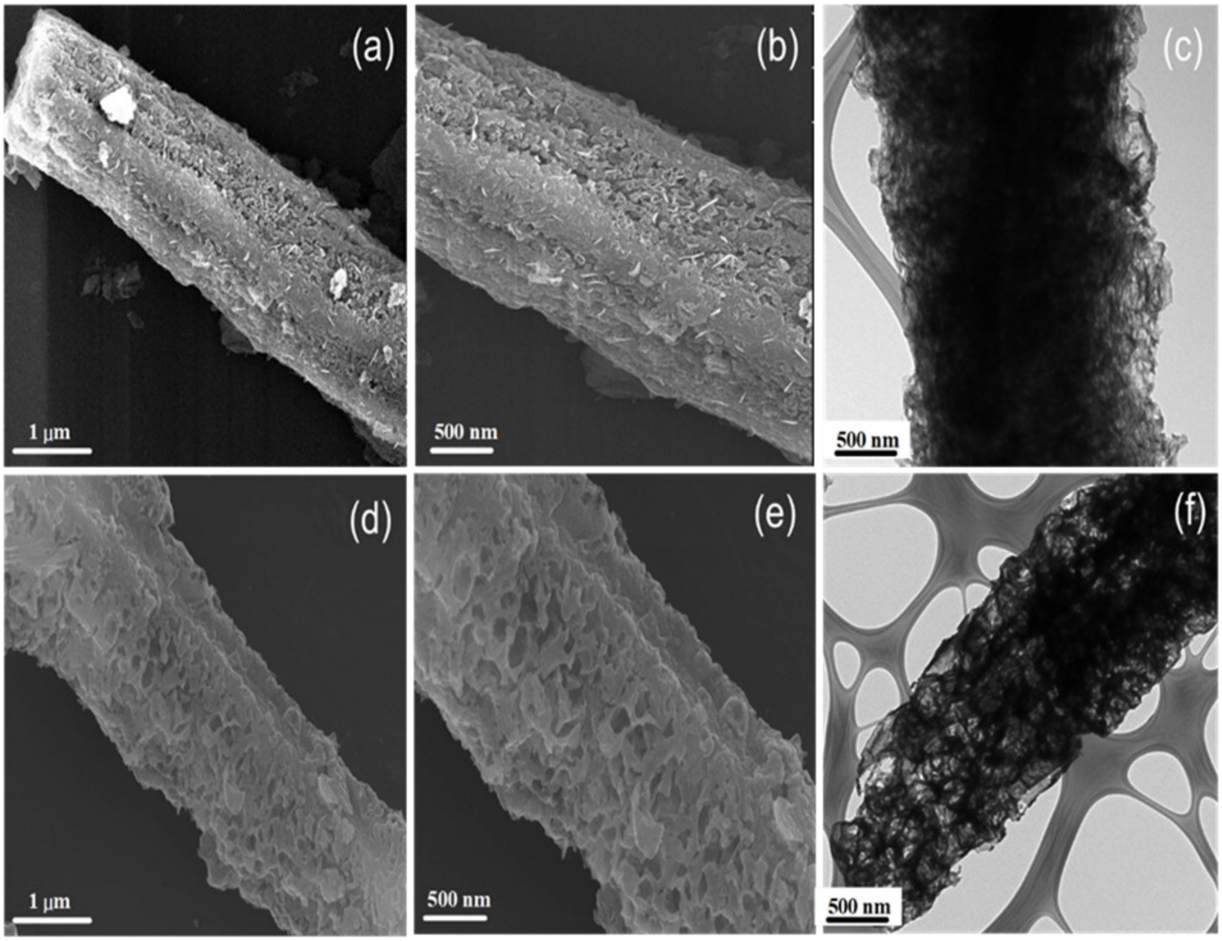

Figure S1. SEM and TEM images of (a, b and c) pure CN and (d, e and f) of S@CN.

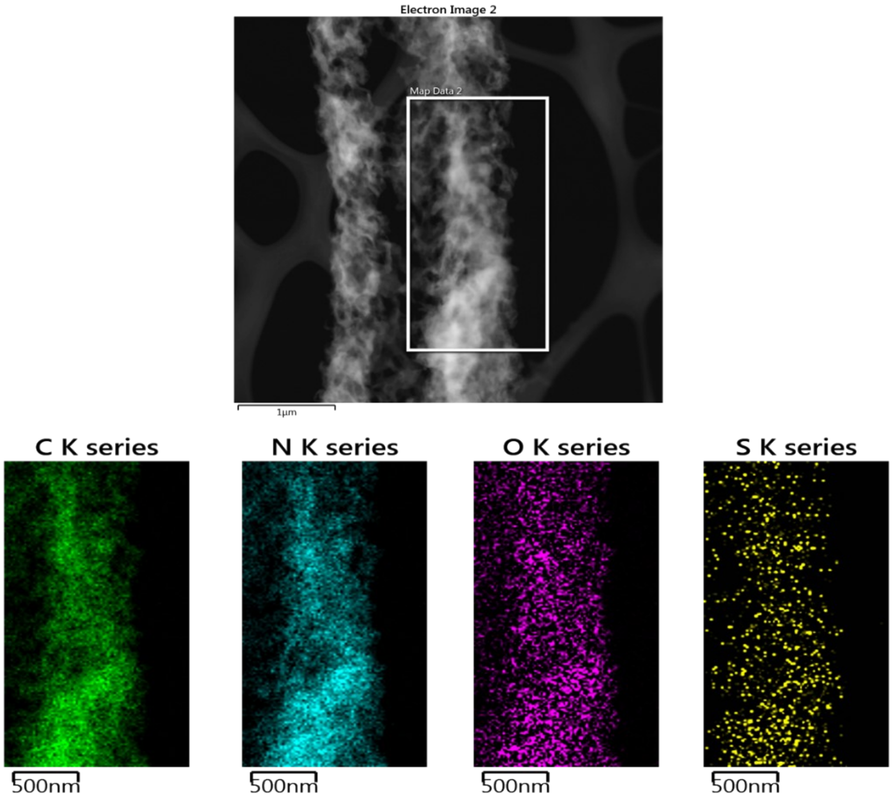

Fig. S2. HAADF-STEM/EDX mapping images of S@CN.

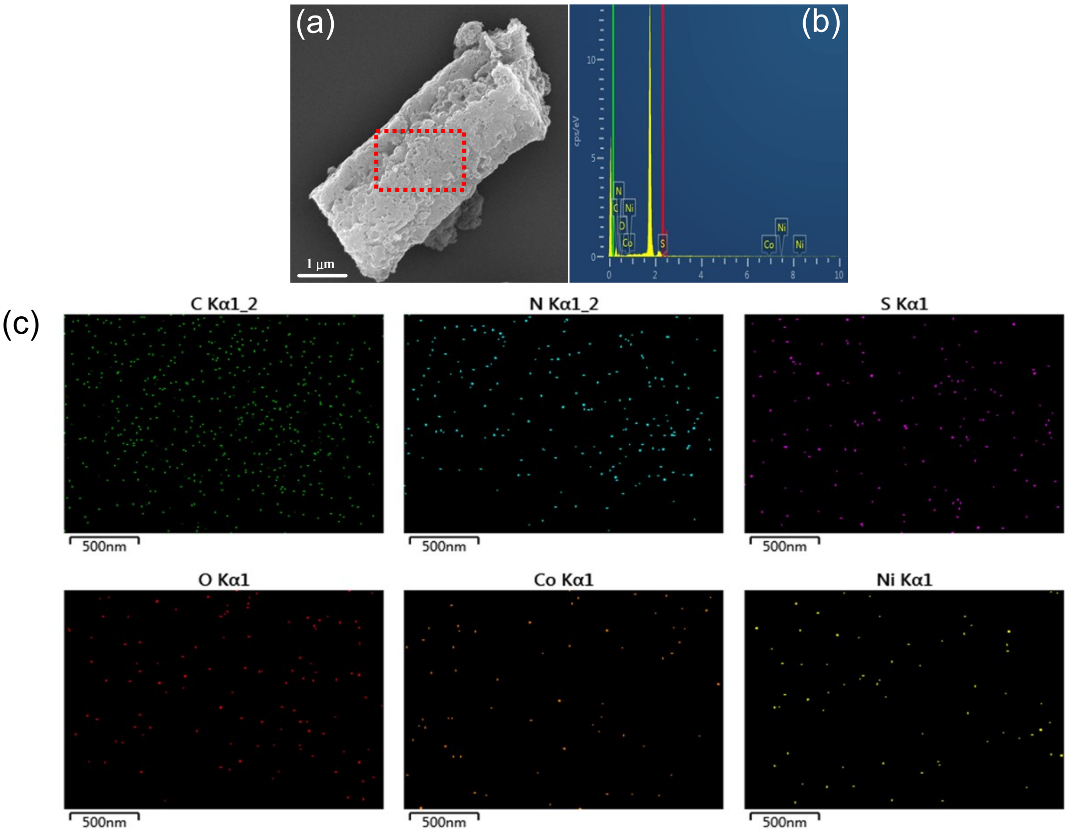

Fig. S3. (a) SEM image, (b) EDS spectrum, and (c) corresponding elemental mapping of NiCo-S@CN.

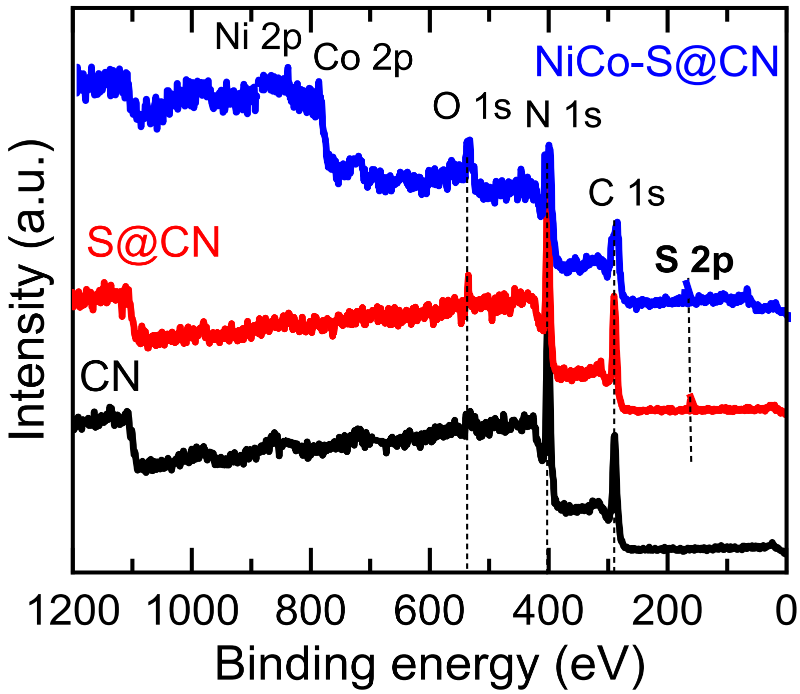

Fig. S4. High resolution XPS survey spectra of synthesized catalysts.

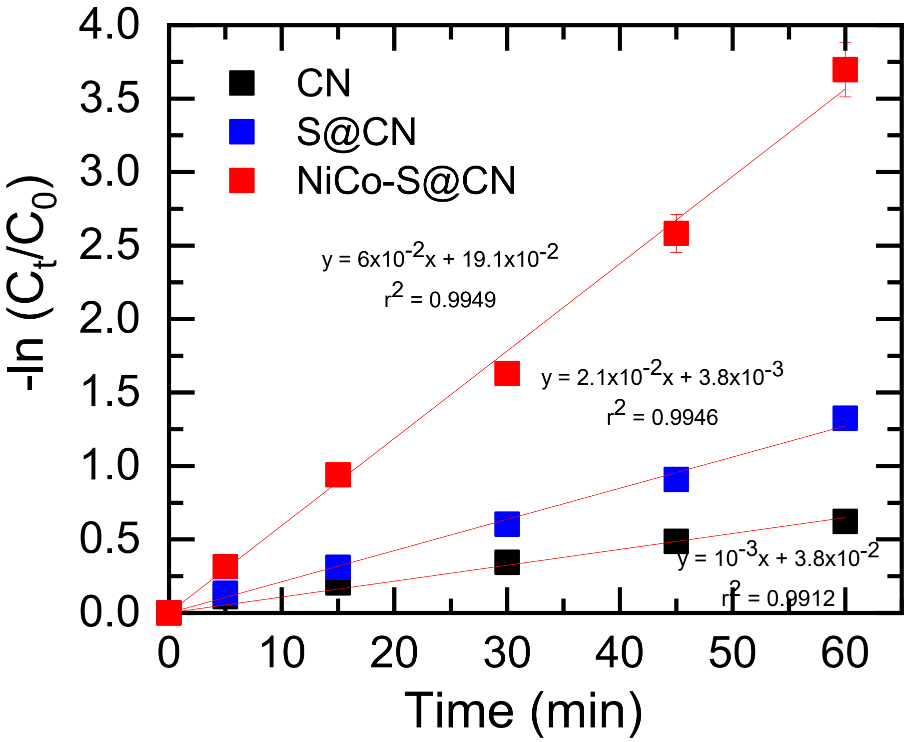

Fig. S5. Kinetic curve data for TC degradation with different photocatalysts under solar light irradiation.

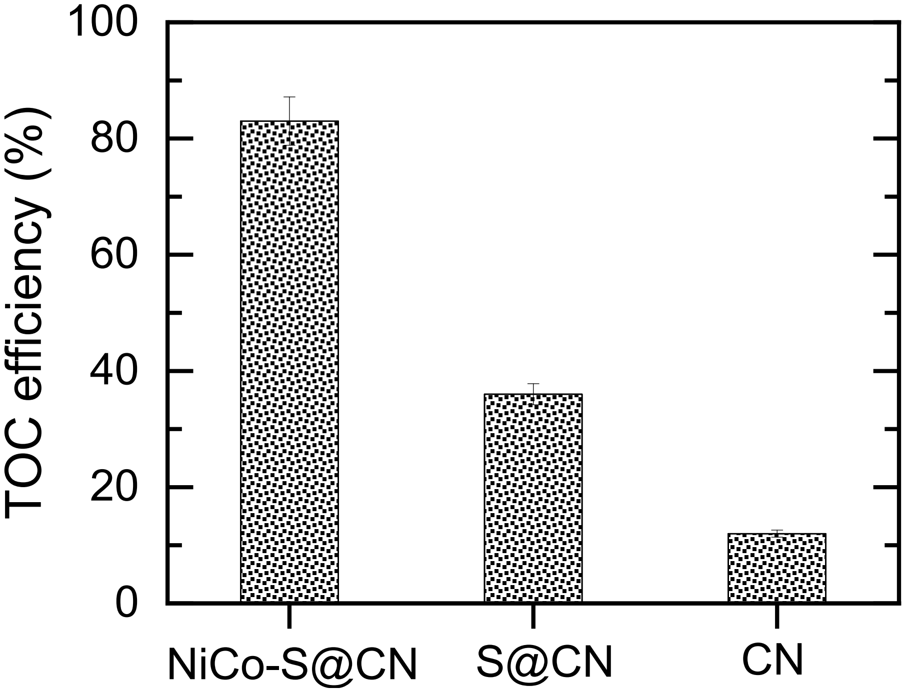

Fig. S6. TOC removal efficiency by different photocatalysts.

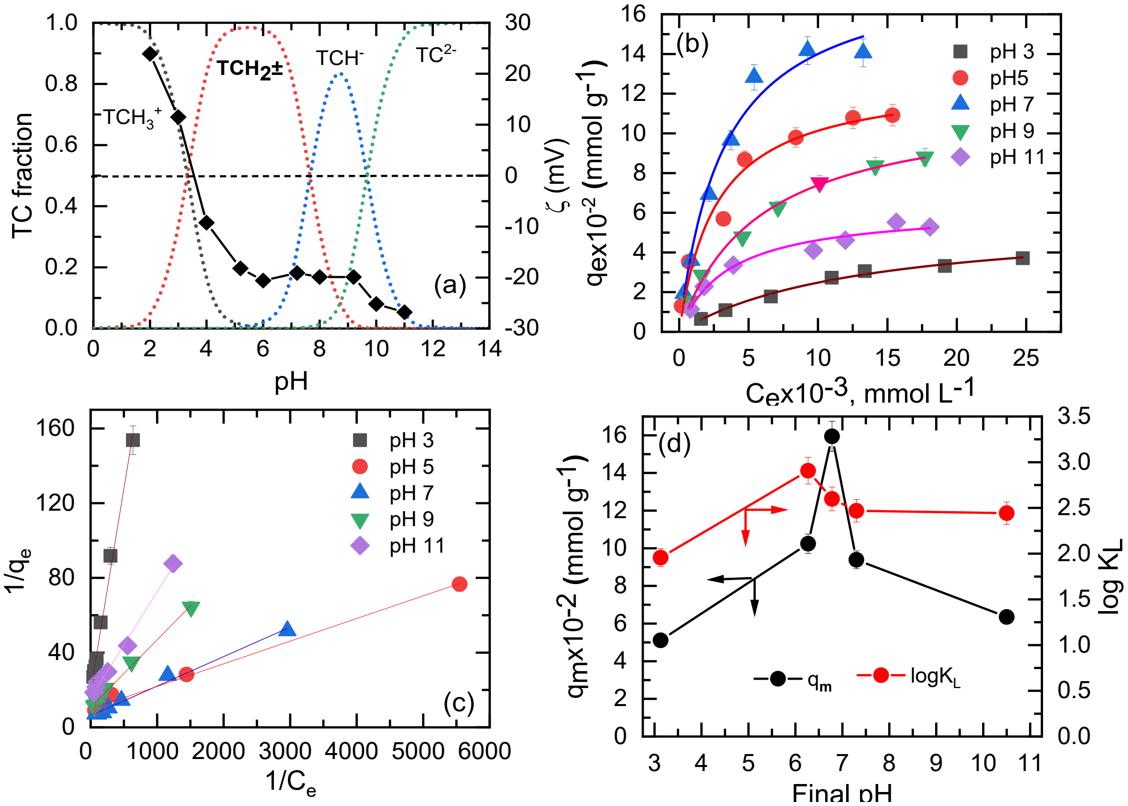

Fig. S7. (a) TC speciation and zeta potential of NiCo-S@CN as function of pH. (b) and (c) Langmuir fitted isotherm of TC adsorption on NiCo-S@CN at various pHs. (c) q_m and $logK_L$ as a function of final pH.

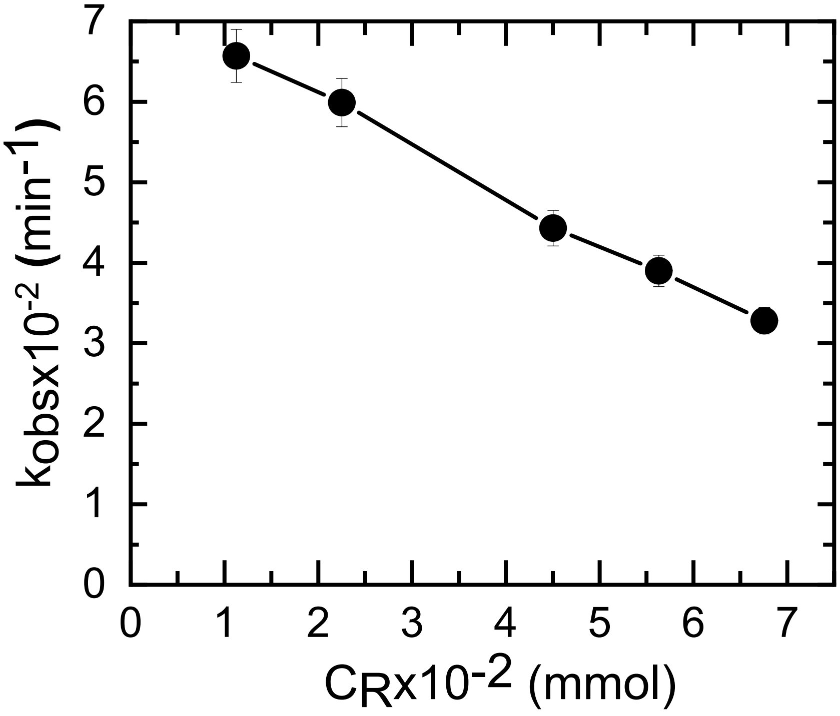

Fig. S8. k_{obs} of TC degradation as a function of initial TC concentration at pH 7.

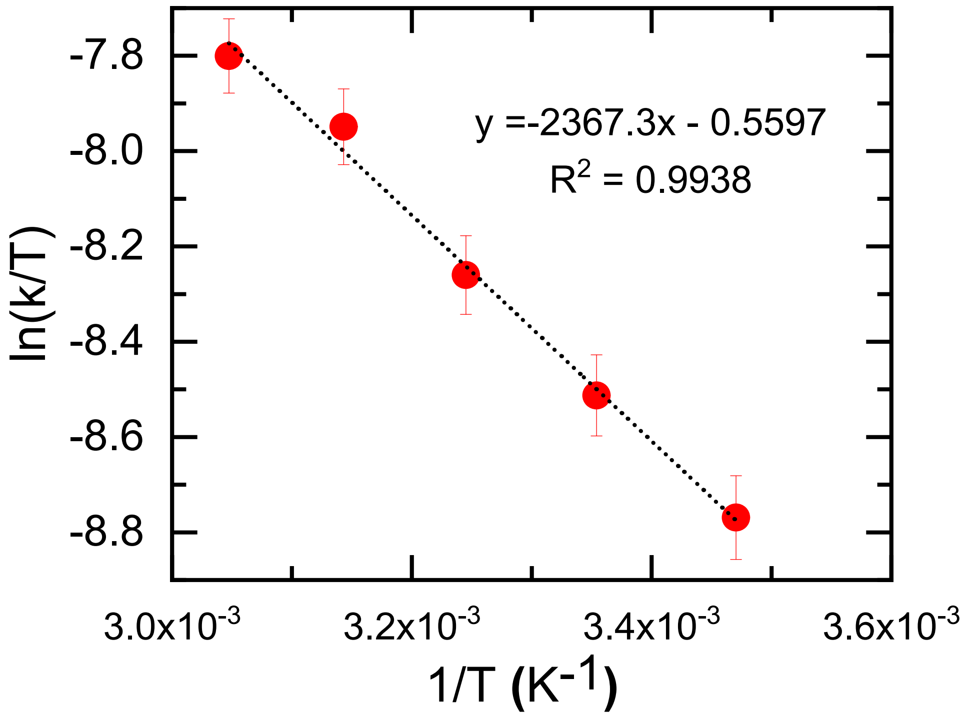

Fig. S9. Eyring plot for the photodegradation of TC.

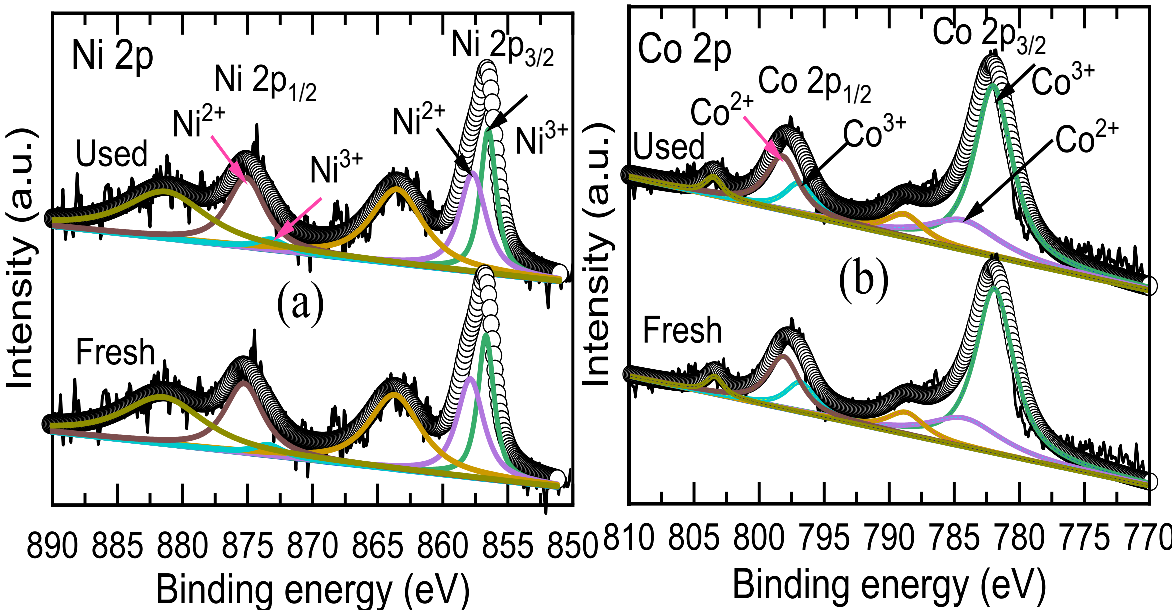

Fig. S10. XPS spectra of (a) Ni 2p and (b) Co 2p before and after use

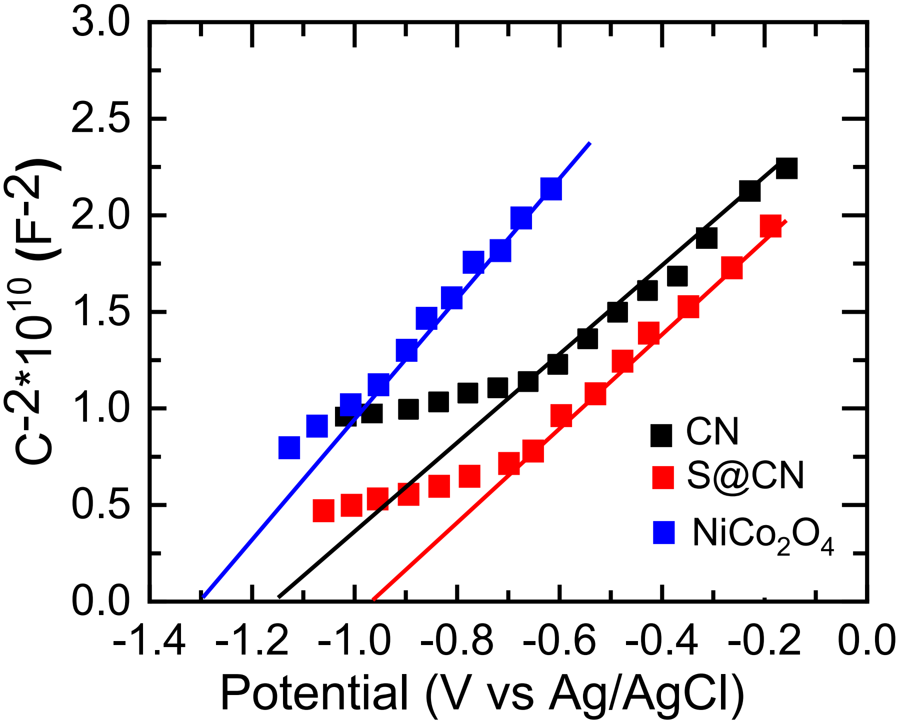

Fig. S11. Mott-Schottky plots of CN, SCN and $NiCo_2O_4$ at selected frequency 1000 Hz.

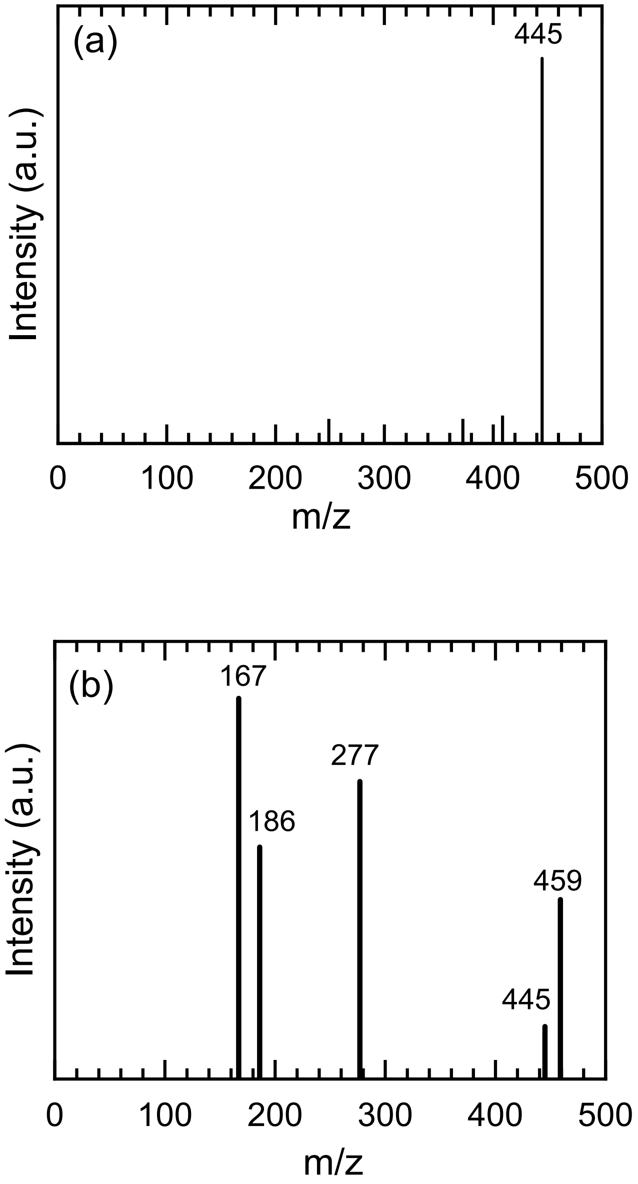

Fig. S12. m/z values of TC degradation (a) before and (b) after photodegradation reaction for 60 min.

Table S1. TC removal by different photocatalysts.

Catalyst	TC (mg L^{-1})	Catalyst dosage (g L^{-1})	Time (min)	Removal efficiency (%)	k_{obs} (min^{-1})	References
NiCo-S@CN	10	0.2	60	> 99	$6x10^{-2}$	This study
MoO_3/Ag/g-C_3N_4	20	0.2	100	96	$1.78x10^{-2}$	1
Co_3O_4/g-C_3N_4	44	0.5	180	97	$1.37x10^{-2}$	5
B doped g-C_3N_4	10	0.2	60	88.1	$2.6x10^{-2}$	11
Ba-doped g-C_3N_4	20	0.2	120	91.94	$1.75x10^{-2}$	37
AgBr/$CuBi_2O_4$	10	0.5	60	90	$2.52x10^{-2}$	42

Table S2. Summary of equilibrium adsorption data fitting from Langmuir model at different pHs.

	q_mx10^{-2} (mmol g^{-1})	K_L (L $mmol^{-1}$)	r^2
pH 3	5.1	90.4	0.9924
pH 5	10.2	806.8	0.9936
pH 7	15.9	397	0.9906
pH 9	9.4	294.3	0.9934
pH 11	6.3	277	0.9930

Table S3. Characteristics of different water matrices.

	Tap water	Lake water
pH	7.18	7.48
TDS	320	542
Conductivity ($\mu\Omega^{-1}$ cm^{-1})	358	426
DOC (mg L^{-1})	2.34	8.53
Na^+	23	30
Ca^{2+}	37	51
Mg^{2+}	16.2	36
HCO_3^-	38	187
Cl^-	5.2	18.4
NO_3^-	-	5.1[a]
SO_4^{2-}	5.34[b]	30.3[b]
Ionic Strength (mM)	4.40	9.82

a: mg-N/L; b: mg-S/L